Prepared discussion

Objekttyp: **Group**

Zeitschrift: **IABSE reports of the working commissions = Rapports des commissions de travail AIPC = IVBH Berichte der Arbeitskommissionen**

Band (Jahr):   **4 (1969)**

PDF erstellt am: **22.05.2024**

DISCUSSION PRÉPARÉE / VORBEREITETE DISKUSSION / PREPARED DISCUSSION

Statistical Concepts in Aseismic Design

Concepts statistiques dans les analyses paraséismiques

Statistische Methoden für den Entwurf bei Erdbeben

M. AMIN   A. H.-S. ANG
Ph.D.   Ph.D.
Department of Civil Engineering
University of Illinois
Urbana, Illinois U.S.A.

INTRODUCTION

In aseismic design, a dynamic analysis is usually required to evaluate the performance of important structures subjected to earthquakes that are likely to occur at a given site. The response of a lightly damped system depends strongly on the history of recorded motions; but since the time histories of future motions corresponding to a given intensity are unpredictable, present seismic design is based on earthquake environments prescribed in the form of a smooth (maximum) response spectrum. The available rules for estimating the responses of multi-degree-of-freedom elastic systems from a given response spectrum, however, are based on heuristic arguments and limited comparisons with results obtained through integration of recorded motions for certain responses [1].* Moreover, these rules do not give a direct procedure for taking the dispersion of the maximum response into account.

A stochastic approach to aseismic design, in principle, could provide a consistent and systematic means for designing against a set (or ensemble) of motions of prescribed intensity. With this approach, all responses of interest can be considered and explicit consideration can be given to the observed dispersions. Recognition of this fact has attracted much attention to the development of stochastic earthquake models [2], and to the formulation of approximate methods for calculating the distribution of maximum response under random earthquake-type motions [3, 4, 5, 6, 7, 8, 9].

For the stochastic approach to be of practical value, however, it is necessary to clarify the earthquake models that should be used and the technique of maximum response evaluation that is adequate for certain categories of structures. For linear structures considered herein, the results obtained thus far are quite encouraging and indicate the feasibility for practical implementation of certain random vibration results to aseismic design.

---

*Bracketed numerals refer to the corresponding references cited.

DISTRIBUTION OF MAXIMUM RESPONSE

Poisson Assumption for Up-Crossings

For structures subjected to earthquake-type ground motions, the exceedance of a high response level can be approximately described as a nonhomogeneous Poisson process with an exceedance rate equal to the rate of the up-crossings. This approximation yields the survival probability as

$$P_s(t) = P \left[\left| X(\tau) \right| < b; \; o \leq \tau \leq t \right] = e^{-2 \int_o^t \nu_b (\xi) \, d\xi} \tag{1}$$

with

$$\nu_b (\xi) = \int_o^\infty \dot{x} \, f_{X,\dot{X}} (b, \dot{x}; \xi) \, d\dot{x} \tag{2}$$

in which $f_{X,\dot{X}}$ is the joint density of the random response of interest X and its derivative $\dot{X}$ at time $t = \xi$. The probability of exceeding the response level $X = \pm b$ at least once within $(0,t]$ is then obtained from

$$P_e(t) = 1 - P_s (t) = 1 - e^{-2 \int_o^t \nu_b (\xi) \, d\xi} \tag{3}$$

If the response is a stationary process throughout $(0,t]$, $\nu_b (\xi)$ becomes a constant $\bar{\nu}_b$; ignoring a small probability of premature failure, Eq. (1) becomes, in this case,

$$\bar{P}_s (t) = e^{-2 \bar{\nu}_b t} \tag{4}$$

Eq. (4), which will be referred to as the homogeneous Poisson approximation, has been applied to the response of single-degree-of-freedom systems by a number of authors [8, 9].

For long durations and high response levels, Eq. (4) is asymptotically correct [10]; otherwise, up-crossings are correlated and the homogeneous Poisson assumption would not strictly be valid. Also, for small values of the integral, Eq. (3) gives results very close to the upper bounds in [5, 7]; however, the homogeneous Poisson assumption may not always provide an upper bound. This is particularly true for small values of t.

To examine the applicability of the Poisson assumption in practical situations of interest, the values of $P_e(t)$ for the displacement response of a linear single-degree-of-freedom system subjected to a base motion described as a Gaussian white noise excitation are compared in Fig. 1 for a system with a 2-second period and for two values of damping, $\beta = 0.02$ and 0.08. For this type of excitation the response and its derivative form a Markov vector and the numerical scheme described in [4] was used to obtain accurate results which are then compared to those obtained from the homogeneous and
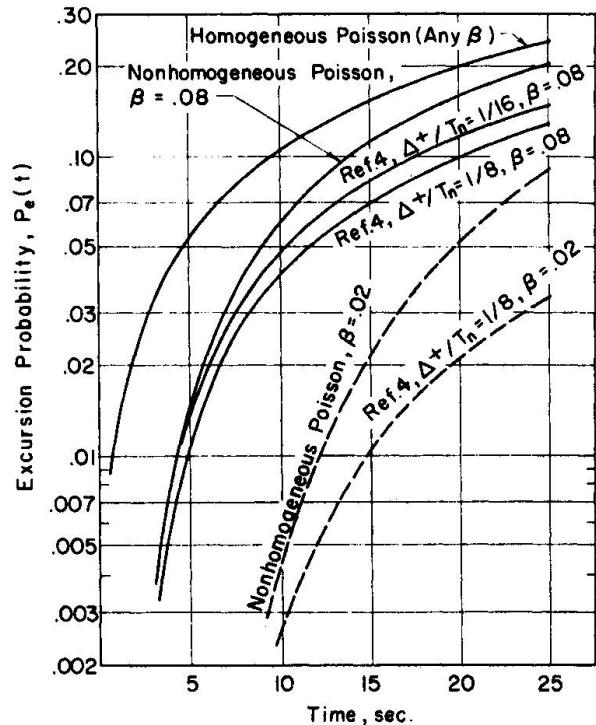

FIG. I COMPARISON OF CALCULATED PROBABILITIES OF EXCURSION — $T_n = 2$ sec. , $b = 3\sigma_0$, WHITE NOISE EXCITATION

nonhomogeneous Poisson assumptions. The response level is $b = 3\sigma_o$, in which σ_o is the rms value of stationary response, i.e.

$$\sigma_o^2 = \frac{\pi S_o}{2\beta\omega_n^3}, \quad \omega_n T_n = 2\pi \tag{5}$$

It is seen that for durations of 25 seconds or so the nonhomogeneous Poisson assumption improves the results over that of the homogeneous Poisson assumption. This is particularly true for the lower damping value. Zero initial conditions were assumed; hence, the response of a 2-second system with 2% damping is quite nonstationary for the durations considered, which is the reason for the need for a nonhomogeneous Poisson procedure. For higher damping values and systems with shorter periods, the difference between the homogeneous and nonhomogeneous processes becomes less significant for durations of the order of 25 seconds.

Another measure of the reasonableness of the above Poisson process approximation can be seen in terms of the response levels corresponding to a specified probability of exceedance P_e in a given duration. For a 2-second system with $\beta = 2\%$ and P_e (25) = 10%, the required response levels are respectively, $3.3\sigma_o$, $3\sigma_o$, and $2.6\sigma_o$ for the homogeneous and nonhomogeneous Poisson approximations, and the accurate Markov scheme of calculation.

Probabilistic Response Spectra

On the basis of Eq. (1) the median pseudo velocities, $V = \omega_n b$ corresponding to P_e (25) = 0.5, computed for a Gaussian excitation with spectral density

$$G_{y_1}(\Omega) = S_{ol} \frac{1 + 4\beta_{f_1}^2 \left(\frac{\Omega}{\omega_{f_1}}\right)^2}{\left[1 - \left(\frac{\Omega}{\omega_{f_1}}\right)^2\right]^2 + 4\beta_{f_1}^2 \left(\frac{\Omega}{\omega_{f_1}}\right)^2}, \quad \begin{array}{l} -\infty < \Omega < \infty \\ \beta_{f_1} = 0.642 \\ \omega_{f_1} = 15.5 \text{ sec}^{-1} \end{array} \tag{6}$$

are compared in Fig. 2 with the average pseudo velocities obtained by Housner [11]. The value of S_{ol} used to compute these results is 0.0052 ft^2/sec^3. In [11, 12], which used simulation techniques to generate member functions from Eq. (6), it was found that $S_{ol} = 0.00614$ ft^2/sec^3 provides a good fit with Housner's spectra. It should be remembered that when using simulation studies, the average spectra calculated do not correspond to a specific value of probability of exceedence; rather, the spectra obtained from a simulation approach are

FIG. 2 SMOOTH VELOCITY SPECTRA

simply the averages of the observed maximum responses at each damping and frequency. Furthermore, in [12] some sensitivity of S_{ol}, required for good fit, to the time interval used for generation of artificial earthquakes was reported. In view of these observations the value of $S_{ol} = 0.0052$ ft^2/sec^3 which gives a good fit between median pseudo velocity spectra and the Housner spectra is
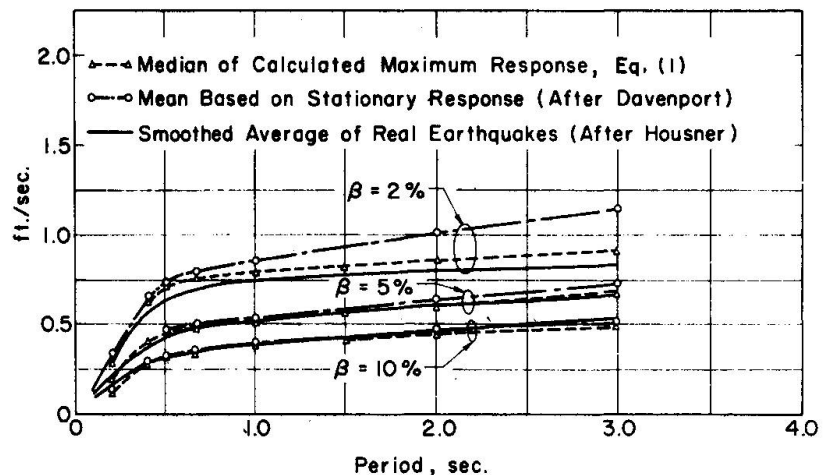
considered to be a good agreement between the Poisson assumption and simulation studies. Of course, by adopting the Poisson process approximation, the tedious process of simulation is avoided.

In Fig. 2 are also shown the mean response values computed from an expression due to Davenport [8], which assumes a homogeneous Poisson process. A duration of 25 seconds was used throughout.

Thus, for purposes of earthquake engineering design of linear systems, the significant maximum response statistics can be adequately determined on the basis of the nonhomogeneous Poisson process described above for a reasonably wide range of frequencies. If the excitation, system period, and damping are such that the nonstationarities in the excitation and response can both be ignored, the exceedance process may also be approximated by a homogeneous Poisson process as has been suggested previously [8, 9].

DESCRIPTION OF GROUND MOTIONS

Influence of Nonstationarity

In Fig. 4 are presented the first-passage time probability density, $f_T(t)$, and reliability function $P_s(t) = 1 - \int_0^t f_T(\tau) \, d\tau$, corresponding to the shot noise and truncated white noise inputs shown in Fig. 3. These results were determined with the computational method of [4] for a system with a 2-second period and $\beta = 0.02$; b = 3 σ_o. The comparison shown in Fig. 4 is of interest because the shot noise excitation has been shown to represent quite well the nonstationarity observed in strong-motion records such as El Centro, Taft, and Olympia [14]. Moreover, it is known that long-period systems are more sensitive to input nonstationarity [12] and that for such systems the earthquake excitations can be treated as an uncorrelated process since the effective correlation time of earthquake motions is approximately 0.1 sec.

The comparison of the probability densities in Fig. 4 shows that the influence of input nonstationarity is controlled by the tail portion of the shot noise; therefore, for long duration responses the computed reliabilities may appreciably be in error. However, for durations of 25 sec. or so which apply to earthquakes of the type considered, the difference in the system reliabilities does not appear to be significant. This is further substantiated by the results of Table 1, which gives the response levels corresponding to an exceedance probability of $P_e(25) = 5\%$ in a 25-second duration.
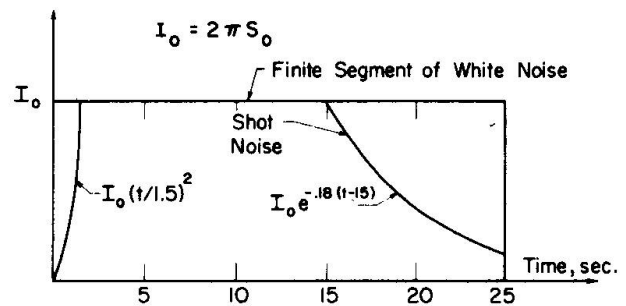
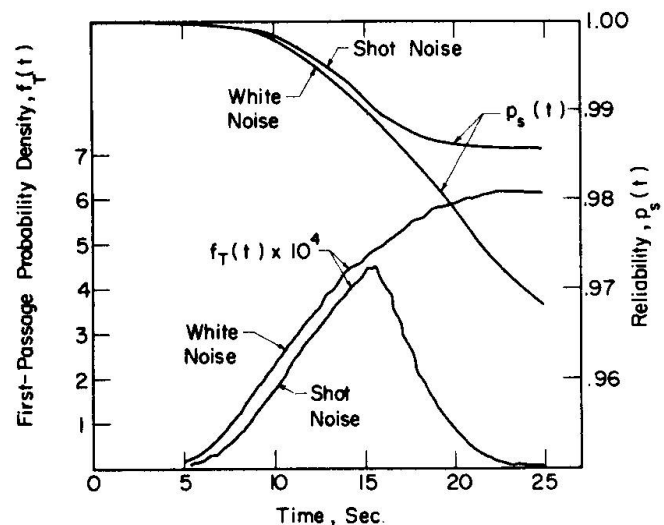FIG. 3 INTENSITY FUNCTIONS FOR UNCORRELATED EXCITATIONS CONSIDERED

FIG. 4 FIRST-PASSAGE TIME PROBABILITY DENSITY AND RELIABILITY FUNCTIONS — — T_n = 2 sec., β = 0.02, b = 3 σ_o, Excitations in Fig. 3

TABLE 1: RESPONSE LEVELS FOR 5% PROBABILITY OF EXCEEDENCE

Elastic systems with 2% damping; duration = 25 sec.

Period, Sec.	Response Values*	
	Shot Noise	White Noise
1	3.00	3.25
2	2.70	2.85
3	2.32	2.60

* Measured in terms of σ_o, Eq. (5)

The insensitivity of the maximum response of linear damped systems to nonstationarity in the earthquakes of the type considered indicates that in specifying the earthquake environment for purposes of probabilistic design of such systems, primary attention should be given to the specification of the input spectral density.

It should be emphasized that the above conclusion is restricted to damped linear systems. Some exploratory results for elasto-plastic systems show that the effect of non-stationarity tends to increase with increasing values of the ductility factor [13].

Definition of Intensity

For dynamic seismic analysis, the earthquake environment is normally defined in terms of a smooth response spectrum; for firm ground conditions, an example would be the Housner's spectra [11]. Simulation studies [14, 15] have also shown that smooth average pseudo velocity spectra may be obtained from the spectral density of Eq. (6) or any of the following:

$$G_{\ddot{Y}_2}(\Omega) = S_{02} \frac{1}{\left[1 - \left(\frac{\Omega}{\omega_2}\right)^2\right]^2 + 4\beta_2^2\left(\frac{\Omega}{\omega_2}\right)^2}, \quad \begin{array}{l} -\infty < \Omega < \infty \\ \beta_2 = 0.5 \\ \omega_2 = 3.14 \text{ sec}^{-1} \end{array} \tag{7}$$

and

$$G_{\ddot{Y}_3}(\Omega) = S_{03}, \quad |\Omega| < 62.8 \text{ sec}^{-1} \tag{8}$$

Fig. 5 shows these spectral densities with S_{oi} determined so that the density amplitudes are the same for periods ranging from 2 to 4 sec. Clearly, the shapes of these densities are not the same. However, the median pseudo velocity spectra computed for the above densities using Eq. (1), and a low damping (β = .02), are fairly close to each other as shown in Fig. 6a. This is in agreement with the findings of simulation studies and indicates that once a smooth response spectrum is selected for design, any of several proposed spectral densities may be used with Eq. (1) and the spectral density amplitude may be obtained from the specified response spectrum values.

FIG. 5 NORMALIZED POWER SPECTRAL DENSITIES

Fig. 6b shows the pseudo velocity spectra obtained from the spectral densities of Eqs. (6), (7), and (8) in which the constants S_{oi} are selected so as to yield the same rms ground acceleration. These pseudo velocity spectra differ from each other.

Therefore, for purposes of consistency in practical aseismic design, the environment should be defined on the basis of a smooth design response spectrum; and from this, a corresponding spectral density can be obtained for use in the stochastic approach.
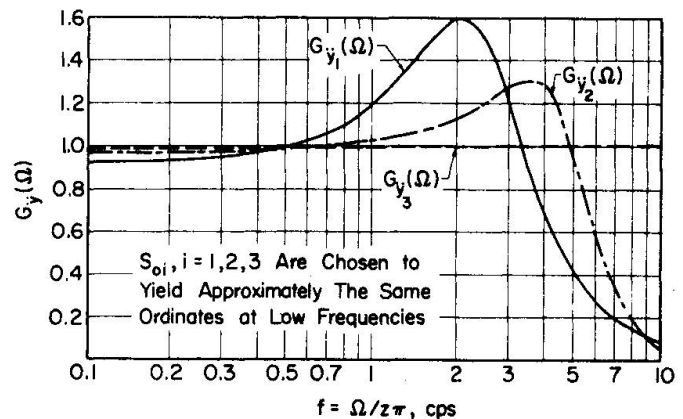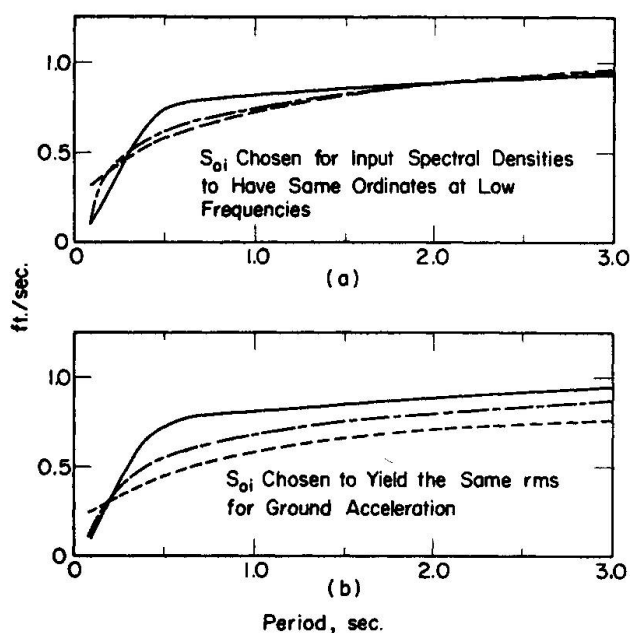
FIG. 6   MEDIAN PSEUDO VELOCITY SPECTRA
CORRESPONDING TO TWO NORMALIZATIONS OF
POWER SPECTRAL DENSITIES— β = 2 %

PRACTICAL IMPLICATIONS

The stochastic approach described above is intended to improve practical design against earthquake forces; the implications are especially significant with reference to the design of multi-degree-of-freedom systems as illustrated below. An important aspect of earthquake motions that seems to be neglected in present designs, or at least is not explicitly considered, is the fact that the response to actual earthquakes of the same intensity has a wide dispersion as will be illustrated in Table 2.

An Illustrative Application

For the purpose of illustrating the practical implications alluded to above, the system shown in Fig. 7 is considered and the relative story distortions are studied. The ratio k/m is selected to give fundamental mode period of 1sec., and 5% damping is used in all the modes. All the 5 modes are considered in the results reported in Table 2, which provides a comparison for three sets of calculations.

TABLE 2:   RESULTS FOR SYSTEM IN FIG. 7

Response x 100. ft. (1)	Normalized Records			Random Vib.		Response Spectrum	
	Average (2)	Range (3)	Second Highest (4)	P_e=.5 (5)	P_e= 0.10 (6)	SRSS (7)	ABS (8)
U_1	353	243 to 587	442	380	434	310	380
(U_2-U_1)	321	216 - 548	402	341	389	282	319
(U_3-U_2)	283	190 - 476	333	290	330	236	292
(U_4-U_3)	221	158 - 351	248	224	251	179	246
(U_5-U_4)	133	109 - 187	152	130	145	102	159

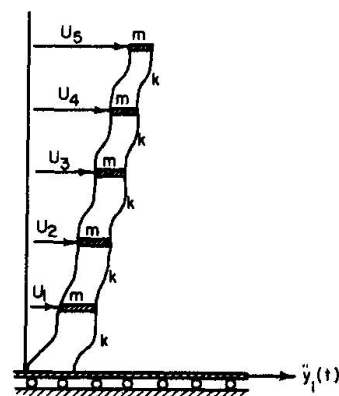
FIG. 7 SYSTEM CONSIDERED

The power spectral density of Eq. (6) is used with S_{01} = 0.0052 ft^2/sec^3. On the basis of Fig. 2, stationary response assumption is acceptable for the period and damping values considered. Assuming Gaussian response, $\bar{v}_b$ of Eq. (4) is

$$\bar{v}_b = \frac{1}{2\pi} \frac{\sigma_{\dot{X}}}{\sigma_X} e^{-\frac{1}{2}(\frac{b}{\sigma_X})^2} \tag{9}$$

in which σ_X and $\sigma_{\dot{X}}$ are the standard deviations of the response X and its derivative $\dot{X}$, respectively. For example, if X is taken to be the second story deformation, then

---

*It has been numerically verified that the coupling effect of modes can be ignored in this structure because of separation in modal frequencies.

$$\sigma^2_X \sim \sum_{k=1}^{5} \gamma^2_k \left[\Phi_k (2) - \Phi_k (1) \right]^2 \int_{-\infty}^{\infty} G_{\dot{Y}_1} (\Omega) \, H^2_k (\Omega) \, d\Omega \tag{10}$$

in which γ_k is the participation factor of mode k, Φ_k (i) is the amplitude of point i in mode k, and H_k (Ω) is the modal frequency response function. The integral in Eq. (10) is adequately approximated by the following:

$$\int_{-\infty}^{\infty} G_{\dot{Y}_1} (\Omega) \, H^2_k (\Omega) \, d\Omega = \begin{cases} \dfrac{\pi \, G_{\dot{Y}_1} (\omega_k)}{2 \beta \, \omega^3_k} \; ; \quad \omega_k \leq 2 \, \omega_{f_1} \\[4mm] \dfrac{\pi \, G_{\dot{Y}_1} (\omega_k)}{2 \beta \, \omega^3_k} + \dfrac{\omega_{f_1} (1 + 4 \beta_{f_1})}{2 \beta_{f_1} \, \omega^4_k} \, \pi \, S_{01} ; \; \omega_k > 2 \, \omega_{f_1} \end{cases} \tag{11}$$

Similar simplifications are possible for $\sigma_{\dot{X}}$.

Results of such calculations are tabulated in columns 5 and 6 of Table 2, representing the median and the 90 percentile response values.

The results for the normalized records, in Table 2, were obtained through a step-by-step integration of the equations of motion for the two horizontal components of the following records: El Centro (1934, 1940), Taft (1952), and Olympia (1949). Before processing, however, the records were normalized, following Housner [11], to have the same area under the undamped spectrum curve (from T = 0.1 sec. to T = 2.5 sec.); the responses thus normalized were averaged and fitted to the Housner's spectrum with zero damping. This gave the appropriate factors by which each record was multiplied and then used to obtain eight different responses for the multi-degree-of-freedom system. The average, the observed range of each response, and the second highest among the eight values are given in columns 2, 3, and 4 in Table 2. For this structure the highest values of all responses came from the same earthquake, NS El Centro 1934, but different records gave second highest values listed for the five response quantities summarized in Table 2.

The results listed under "response spectrum," columns 7 and 8 of Table 2, were obtained using the median response spectrum of Fig. 2 with β = 5%. The absolute sum (ABS) and the square root of sum of the squares (SRSS) of the peak modal responses thus obtained are given in the columns indicated.

Discussion

For the example structure, almost all of the response U_1 (measure of base shear) is due to the first mode whereas the higher modes increase in importance for the response U_5-U_4. With this in view, the agreement between the U_1 responses in columns 2 and 5 merely indicates that a reasonable normalization of the records has been achieved since it is intended that the collection of records and earthquake model used produce roughly the same average effect on a single-degree-of-freedom system. On the other hand, the agreement between the $(U_5 - U_4)$ values in columns 2 and 5 verifies the applicability of Eq. (1) to multi-degree-of-freedom systems.

Clearly there is a wide range in the responses of the structure to the normalized records; the proposed stochastic procedure with proper selection of P_e provides a consistent means for taking this range into account.

The values in columns 7 and 8 should be compared with those in column 5 because these are all responses to the same average base motion, described by the median response spectrum in Fig. 2. Note that the values of column 7 consistently underestimate those of column 5 whereas the values of column 8 are not consistent for all the responses in the structure.

CONCLUSIONS

The main conclusions of the paper may be summarized as follows:

1.   The Poisson approximation for up-crossings, Eq. (1), provides a flexible means for obtaining maximum response statistics under random earthquake-type motion; for single-degree-of-freedom systems, the differences with theory are not large enough to be significant, Fig. 1, and the results thus obtained are in agreement with those from simulation studies, Fig. 2. For the multi-degree-of-freedom system considered, Eq. (1) appears to produce results in fair agreement with those obtained from a normalized set of recorded accelerograms.

2.   Responses to a set of normalized recorded motions having the same average response spectrum, which are commonly pooled together, vary in a wide range, Table 2. Unless quantitative means become available to separate differences among these records, it is necessary to take this variability into account. A random vibration approach provides a consistent manner for implementing this goal in practice.

3.   For damped linear systems, the influence of nonstationarity of the input motions analogous to El Centro, Taft, and Olympia records can be ignored, Table 1. Starting from an average smooth response spectrum it is then possible to arrive at an appropriate spectral density to be used in a stochastic procedure for design.

ACKNOWLEDGMENT

REFERENCES

1.   Rosenblueth, E. and Elorduy, J. "Responses of Linear Systems to Certain Transient Disturbances," Proc. 4WCEE, Chile (1969).

2.   Recent papers can be found in Proc. 4WCEE, Session A1, Chile (1969).

3.   Rosenblueth, E. and Bustamente, J. L., "Distribution of Structural Responses to Earthquakes," Proc. ASCE, Vol. 88, EM3 (1962).

4.   Crandall, S. H., Chdndiramini, K. L., and Cook, R. G., "Some First Passage Problems in Random Vibration," J. Appl. Mech., Vol. 33, No. 3, (1966).

5.   Shinozuka, M., "Probability of Structural Failure Under Random Loading," Proc. ASCE, Vol. 90, EM 5 (1964).

6.   Roberts, J. B., "An Approach to the First-Passage Problem in Random Vibration," J. Sound Vib., Vol. 8, No. 2 (1968).

7.   Bolotin, V. V., "Statistical Methods in Structural Mechanics," STROIIZDAT, Moscow, 1965, (Russian).

8.   Davenport, A. G., In Discussion of Ref. 11, Proc. ASCE, Vol. 90, EM5 (1964).

9.   Pereira, J. M. M., "Behavior of an Elasto-Plastic Oscillator Acted by Random Vibration," Proc. 3WCEE, New Zealand (1965).

10.   Cramer, H. and Leadbetter, M. R., Stationary and Related Stochastic Processes, John Wiley and Sons, Inc. (1967).

11.   Housner, G. W., and Jennings, P. C., "Generation of Artificial Earthquakes," Proc. ASCE, Vol. 90, EM1 (1964).

12.   Penzien, J., and Liu, S.-C., "Nondeterministic Analysis of Nonlinear Structures Subjected to Earthquake Excitations," Proc. 4WCEE, Chile (1969).

13.   Amin, M., Ts'ao, H.-S., and Ang, A. H.-S., "Significance of Nonstation-
       arity of Earthquake Motions," Proc. 4WCEE, Chile (1969).
14.   Amin, M., and Ang, A. H.-S., "Nonstationary Stochastic Model of Earth-
       quake Motions," Proc. ASCE, Vol. 94, EM2 (1968).
15.   Bycroft, G. N., "White Noise Representation of Earthquakes," Proc. ASCE,
       Vol. 86, EM2 (1960).

SUMMARY

       Responses to a set of normalized recorded motions vary in a
wide range. It is shown that for linear systems, approximate but
adequate methods are available for systematically applying a
stochastic approach to aseismic design. For certain commonly used
accelerograms nonstationarity of the motions can be ignored when
considering linear systems; in these cases the spectral density
to be used should be selected after a design intensity is defined
by a smooth response spectrum.

RESUME

       Le comportement d'un système soumis à un ensemble normalisé
de mouvements enregistrés varie énormément. Il est démontré que,
pour les systèmes linéaires, il existe des méthodes approximatives
mais adéquates pour appliquer systématiquement l'approche stocha-
stique dans les analyses paraséismiques. La non-stationarité des
mouvements peut être négligée pour certains accélérogrammes large-
ment utilisés et appliqués aux systèmes linéaires. Dans ces cir-
constances, la densité spectrale utilisée doit être déterminée
à l'aide de l'intensité définie par une réponse spectrale lisse.

ZUSAMMENFASSUNG

       Das Verhalten eines Systems gegenüber einer Reihe von beobach-
teten und normalisierten Bewegungen variiert über einen weiten
Bereich. Es wird gezeigt, dass für lineare Systeme ausreichende
Näherungsmethoden vorhanden sind, um systematisch stochastische
Methoden auf den Entwurf von Konstruktionen gegen Erdbebenbean-
spruchung anzuwenden. Für bestimmte, häufig verwendete
Beschleunigung-Zeit-Beziehungen kann für lineare Systeme die Ver-
änderung des Ruhepunktes der Bewegungen vernachlässigt werden. In
diesen Fällen sollten die zu verwendenden Spektraldichten (PSD)
gewählt werden, nachdem die Intensität durch ein ausgeglichenes
Verhaltenspektrum definiert ist.

Leere Seite

Blank page

Page vide

Statistical Evaluation of Load Factors in Structural Design

Calcul statistique des coefficients de sécurité dans la conception des ouvrages

Statistische Berechnung von Sicherheitsfaktoren im Entwurf

WILSON H. TANG
Assistant Professor
of Civil Engineering
University of Illinois

HARESH C. SHAH
Associate Professor
of Structural Engineering
Stanford University

JACK R. BENJAMIN
Professor
of Structural Engineering
Stanford University

I Introduction

The current design procedures in structural engineering involve the use of load factors to account for uncertainties that may exist in the applied loads and in the resisting strength of the structural members. The associated level of reliability depends on the probabilistic character of both loads and resistance. A procedure leading to the determination of load factors is formulated based on the following criteria: 1) The load factors should provide a desired level of structural safety with respect to all loading configuration. 2) This desired level of reliability may be determined by economic factors such as cost of construction and the cost of failure of the structural system. 3) Load factors for individual element design may be determined by the desired level of reliability of the whole system. 4) Additional information about the loading environment and the material strength characteristics can be systematically incorporated into the procedure to obtain a better set of load factors. 5) The procedure to evaluate load factors should be simple in form and easy for application. In the formulation that is presented here, dead, live, wind and earthquake loads are included. First, the load factors for a given reliability level for a structural element are calculated and second, the optimal reliability level of the structural system, its relationship with element reliability and the economic considerations in determining optimal reliability are considered. Step by step procedure is outlined and numerical example is worked out to illustrate the simplicity of the procedure.

II Determination of Load Factors for Dead, Live, Wind and Earthquake Loads

In addition to dead and live load, a structure may be subjected during its life span to loads like earthquake and wind. In previous works, Tang (7), Niyogi (3), Shah and others (4) have initiated such studies under dead and live loads. Incorporation of high wind loads and earthquake loads are especially important for structures with long service life and located around regions where occurrences of earthquakes or hurricanes or both are frequent. Given the location and the desired life span of a structure, the maximum magnitude of earthquake and wind loads that will act on the structure are random variables. In the formulation presented here, only the largest magnitudes of wind and earthquake loads are considered. The effects of repeated occurrences of minor

earthquakes and hurricanes are neglected. If we exclude the possibility that earthquake and wind would occur at the same time, then the possible loading configurations are:

$$W_1 = DL + LL \; ; \quad W_2 = DL + WL \; ;$$
$$W_3 = DL + EL \; ; \quad W_4 = DL + LL + WL \; ;$$
$$W_5 = DL + LL + EL \; .$$

1

where DL, LL, EL and WL represent dead, live earthquake and wind loads respectively. If the mean values of these loads are taken as nominal loads to which load factors are multiplied, the corresponding design load values are:

$$W_1^* = \alpha_{11}\mu_1 + \alpha_{12}\mu_2 \; ; \quad W_2^* = \alpha_{21}\mu_1 + \alpha_{23}\mu_3$$
$$W_3^* = \alpha_{31}\mu_1 + \alpha_{34}\mu_4 \; ; \quad W_4^* = \alpha_{41}\mu_1 + \alpha_{42}\mu_2 + \alpha_{43}\mu_3$$
$$W_5^* = \alpha_{51}\mu_1 + \alpha_{52}\mu_2 + \alpha_{54}\mu_4$$

2

where μ_1, μ_2, μ_3 and μ_4 are the mean dead, live, wind and earthquake loads respectively. Note that load factors

$$\alpha_{13} = \alpha_{14} = \alpha_{22} = \alpha_{24} = \alpha_{32} = \alpha_{33} = \alpha_{44} = \alpha_{53} = 0$$

3

In general, for the ith combination of loading, we can write:

$$W_i^* = \sum_{j=1}^{4} \alpha_{ij}\mu_j$$

4

Stochastically, if all the load components are assumed normally distributed, the design load for the ith loading configuration is

$$W_i = \mu_{W_i} + k_i \sigma W_i = \sum_j \mu_j + k_i \Big(\sum_j \sigma_j^2 + \sum_{\substack{k,\ell \\ k \neq \ell}} \rho_{k\ell}\sigma_k\sigma_\ell\Big)^{1/2}$$

5

where $\rho_{k\ell}$ denotes the coefficient of correlation between the k-th and ℓ-th component. The index j depends on the ith loading configuration. Thus,

$$j = 1,2 \quad \text{when } i = 1 \; ; \quad j = 1,4 \quad \text{when } i = 3$$
$$j = 1,3 \quad \text{when } i = 2 \; ; \quad j = 1,2,3 \quad \text{when } i = 4$$
$$j = 1,2,4 \quad \text{when } i = 5 \; .$$

6

In terms of the component loads, this design load may also be written as

$$W_i = \sum_j \ell_{ij} = \sum \mu_j (1 + k_i V_j)$$

7

where V_j = coefficient of variation of the jth load component. Equating 4, 5 and 7 and assuming that the resistance is Gaussian with coefficient of variation V_R and reliability coefficient k_i, (k_i measures the number of standard deviations in the standardized Gaussian distribution corresponding to the ith load), a general expression for the load factor can be obtained

$$\alpha_{ij} = \frac{1}{1-k_i V_R} \cdot \frac{\ell_{ij}}{\mu_j} = \frac{1 + \dfrac{(\sum_j \sigma_j^2 + k\sum_{\substack{k,\ell \\ k \neq \ell}} \rho_{k\ell}\sigma_k\sigma_\ell)^2}{\Sigma\sigma_j} k_i V_j}{1 - k_i V_R}$$

8

If k_i^* denotes the level of the overall reliability for the ith loading combination, the relation between k_i and k_i^* can be shown to be (ref. 7)

$$k_i = \frac{\sqrt{(V_R \mu_R)^2 + \sigma_{L_i}^2}}{V_R \mu_R + \sigma_{L_i}} \, k_i^* \qquad\qquad 9$$

where

$$\sigma_{L_i} = \left(\sum_j \sigma_j^2 + \sum_{\substack{k,\ell \\ k \neq \ell}} \rho_{k\ell} \sigma_k \sigma_\ell\right)^{1/2} \qquad\qquad 10$$

For any desired level of overall reliability corresponding to k_i^*, k_i is determined from equation 9. Load factors are then computed by equation 8. In order to test for the sensitivity with respect to the type of distribution that is assumed, Extreme Type II (largest value) distribution has been assumed for the wind and earthquake loads, keeping the dead load and live load distributions Gaussian. It was observed that the values of design loads and load factors obtained for any desired reliability level does not change appreciably from the all-Gaussian model.

III **Summary of Procedure**

A step by step procedure is outlined below for the evaluation of load factors under dead, live, wind and earthquake loads. (1) Compute the magnitudes of dead, live, wind and earthquake loads acting on the structure, based on the empirical formula in the existing code. (2) Through structural analysis, obtain the design moments (stresses) due to each load component. Select the critical section for the member to be designed. (Numerical example is given in section 6.) Let μ_1, μ_2, μ_3 and μ_4 be values of such design moments (stresses) at the critical section due to dead, live, wind and earthquake load respectively. (3) Based on the available data, determine the coefficients of variation V_1, V_2, V_3 and V_4 for each load component. Compute σ_1, σ_2, σ_3 and σ_4 by using equation $\sigma_1 = \mu_i V_i$, $i = 1,2,3,4$. (4) From available data, determine coefficient of variation of resistance (V_R). (5) Choose the value of the overall reliability for the member to be designed, say $\bar{u}$. Determine the corresponding reliability coefficient k^* from tables of normal integrals. (6) Compute the values of σ_s, μ_s, σ_L, V_L and k for each loading configuration. All ρ_{ij} except ρ_{14} may be assumed to be zero. The value of each k_i (1 = 1 to 5) is determined from the values k^*, V_R and V_L, by using equation 9 or from charts similar to that in Figure 4. (7) For each loading configuration i, compute load factors α_{ij} by

$$\alpha_{ij} = \frac{1 + \left(\frac{\sigma_L}{\sigma_s} k V_j\right)_i}{1 - k_i V_R}$$

Note that α_{13}, α_{14}, α_{22}, α_{24}, α_{32}, α_{33}, α_{44}, α_{53} are zero. (8) Compute the design load

$$W_i = \sum_{j=1}^{4} \alpha_{ij} \mu_j \quad i = 1 \text{ to } 5 .$$

The example given in Section 6 would help to illustrate the above procedures.

IV **System Analysis**

In general, a structure is made up of structural components called members or elements. For a floor system consisting of four T-beams, each beam is called an element. The reliability of the floor system depends on the reliability of

each beam as well as the type of framing of the system. We will consider two types of systems, namely series system and parallel system.

(A) <u>Series System</u> - The series system is defined as one which fails if any one of its elements fails. When any element fails, that is, when its strength capacity is exceeded by the applied load, it does not continue to deform sufficiently so that its adjacent elements can take on the extra load. If we further assume for the four-beam floor system that (i) The probabilistic properties of each T-beam are identical. (ii) The event that any one beam fails is independent of that of the others. (iii) The loads are evenly distributed to each beam. Then the probability of failure of the floor system is

$$p_{FS} = 1 - (1 - p_F)^4 \approx 4p_F \quad \text{(for small } p_F) \qquad 11$$

where p_F = probability of failure of each element. This may be generalized such that for a series structural system of N elements, its probability of failure is N times that of the individual element, that is

$$p_{FS} = N \cdot p_F \qquad 12$$

(B) <u>Parallel System</u> - On the other hand, if all the elements are designed with sufficient ductility such that they do not lose their load capacity until all elements reach ultimate conditions, the structural system is called a parallel system. Ideally, this system will fail when all the elements fail. However in practice, even for the most ductile system, the structural system will fail when only a fraction of the total number of elements fails. In addition to the assumption listed in Case (A), if we assume for the same floor system that the system will fail if two or more beams fail, then using the concept of Bernoulli Trials,

$$p_{FS} = \binom{4}{2}p_F^2(1 - p_F)^2 + \binom{4}{3}p_F^3(1 - p_F) + \binom{4}{4}p_F^4 \qquad 13$$

For small value of p_F, then

$$p_{FS} = \binom{4}{2}p_F^2 = 6p_F^2 \qquad 14$$

This may be generalized for a parallel structural system with N elements, if the failure of M or more elements lead to system failure, then the probability of system failure is approximately

$$p_{FS} \approx \binom{N}{M}p_F^M \qquad 15$$

Since reliability is defined as

$$\overline{u}_S = 1 - p_{FS} \quad , \quad \overline{u} = 1 - p_F \qquad 16$$

we can see from equations 12 and 15 that simple relations do exist between system reliability and element reliability.

V Cost Analysis

It is known that the total design load increases as the desired level of reliability for one design increases. If we assume that cost of construction is linearly proportional to this value of design load, and let c_2 be the loss when the structure fails, and assume all other costs negligible, an expected total cost function can be defined as

TC = cost of construction + expected cost of failure

$$= c_1 W^*(\overline{u}) + c_2(1 - \overline{u}_S) \qquad 17$$

where W^* = total design load which is a function of reliability; c_1 = construction cost per unit design load for the system; and $\overline{u}$ = reliability of an element.

For a series structural system, applying Equations 12 and 16, this becomes

$$TC(\bar{u}) = c_1 [W*(\bar{u}) + C(1 - \bar{u})] \qquad\qquad 18$$

where $C = \dfrac{\text{cost of failure}}{\text{cost of construction per element per unit design load}}$

In other words, the cost coefficient C is a measure of how important the consequences of structural failure are relative to the unit cost of construction. Thus, a large value of C corresponds to a case where failure involves great losses. In the numerical work which follows, the mean dead load is assumed not as a constant but to be 1 psf per 5 psf of the total design load. The expected total cost function is evaluated for the sample data used for the Gaussian model. Figure 1 shows, for a given value of C, that a distinct minimum cost does exist at a certain level of reliability. As C increases, the optimal design should have a higher level of reliability so that the expected loss due to failure is decreased. The optimal reliability level as a function of the cost coefficient for various coefficients of variation of loads and resistance is shown on Figure 2. The variation in the load does not seem to affect this optimal relation. However as the coefficient of variation of resistance increases, the optimal reliability level does decrease for any given cost coefficient C. This implies that the optimal decision, when the resistance is highly uncertain, is to cut back the cost of construction by using smaller load factors and to risk a higher probability of failure. The analysis is similar in the case of a parallel system. The total cost function for the four-beam floor system example is computed to be

$$TC(\bar{u}) = c_1 [W*(\bar{u}) + 1.5C(1 - \bar{u})^2] \qquad\qquad 19$$

The relation between the cost coefficient and the optimal level of element reliability is given in Figure 3 for various values of the coefficient of variation of the resistance. This relation is again very insensitive to the statistical variation in the applied loads. For a given value of cost coefficient C, the optimal level of element reliability is much less for the parallel system than for the series system. Therefore, for the two types of systems, namely, series and parallel, once we know the values of C and V_R, the optimal level of reliability for element design may be easily determined.

VI Numerical Example - Dead, Live, Wind and Earthquake Loads

A one-story plane frame structure is chosen to illustrate how load factors can be determined in a step by step procedure for a desired level of reliability. The frame's dimension and member stiffness are shown in Figure 5. Assume that only bending moment failure is of interest. (1) Compute the magnitudes of dead, live, earthquake and wind loads acting on the structure. Assume a tributary span of 20 feet perpendicular to the frame. The dead load is represented by a uniform load acting on the girder BC. Its magnitude is given by

w_1 = DL x 20' = 60 x 20 = $1.2^{K/ft}$. Similarly, the magnitude for the live load

is w_2 = LL x 20' = 80 x 20 = $1.6^{K/ft}$. For the earthquake load, the Seismic

Engineering Association of California (SEAOC) recommends the following equation for the equivalent static lateral load. (Ref. 8)

$$Q = KC_o W_o Z_o \qquad\qquad 20$$

We may assume Z_o = 1 (in California), D = 1 for the type of framing and C_o = 0.1 for a one-story structure. Then Q_1 = DL x floor area x Z_o x K x C_o = 60 x 20 x 20 x 1 x 1 x 0.1 = 2.4^K. For the wind load, an equivalent static force is given by (ref. 9)

$$F = .00256 \ Cd \ AV^2 \qquad\qquad 21$$

We may assume $C_d = 1$ for flat wall, $V = 80$ mph for a 50-year occurrence period in San Francisco for a building height of 50 feet, and $A = 10 \times 20 = 200$ square feet for a tributary span of 20 feet and an exposed height of 10 feet. Then $Q_2 = .00256 \times 1 \times 200 \times 80^2 = 3.3^k$. (2) Compute bending moments due to each load. The moments (in kip-ft.) at critical locations are

	DL	LL	EL	WL	DL+LL	DL+EL	DL+WL	DL+LL+EL	DL+LL+WL
A	13.4	18.0	34.3	47.1	31.4	47.7	60.5	65.7	78.5
B	-26.7	-35.7	-25.7	-35.4	-62.4	-52.4	-62.1	-88.1	-97.8 *
C	-26.7	-35.7	27.7	35.4	-62.4	- 1.0	8.7	-36.7	-27.0
D	13.4	18.0	-34.3	-47.1	31.2	-17.9	-33.7	- 3.1	-15.9
E	33.3	44.5	0	0	77.8	33.3	33.3	77.8	77.8

Take location B for our further analysis. (3) Compute mean and standard deviation for each component.

$$V_3^2 \approx V_{z_o}^2 + V_{k_o}^2 + V_{c_o}^2 + V_{w_o}^2$$

$$= (0.1)^2 + (0.08)^2 + (0.2)^2 + (0.08)^2 = 0.0628 \text{ (say)}$$

$$\mu_1 = 26.7 \qquad V_1 = 0.083 \qquad \sigma_1 = 2.22$$
$$\mu_2 = 35.7 \qquad V_2 = 0.25 \qquad \sigma_2 = 8.93$$
$$\mu_3 = 35.4 \qquad V_3 = 0.2 \qquad \sigma_3 = 7.08$$
$$\mu_4 = 25.7 \qquad V_4 = 0.25 \qquad \sigma_4 = 6.43$$

The index 1, 2, 3, 4 correspond to dead, live, wind and earthquake load contributions respectively. The values of the coefficient of variation V_1, V_2, V_3, V_4 are assumed for numerical illustration. The correlation coefficients ρ_{ij} are assumed zero, except for $\rho_{14} = 0.5$. (4) Assume coefficient of variation of resistance, say, 0.1 in this case. (5) Choose the desired overall reliability $u = 0.9999$. (6) Compute the values of σ_s, μ_s, σ_L, V_L, k^*, k.

Case	Loading Combination	σ_s	μ_s	σ_L	V_L	k^*	k
1	DL + LL	11.15	62.4	9 2	0.147	3.72	2.68
2	DL + WL	9.3	62.1	7.41	0.12	3.72	2.7
3	DL + EL	8.65	52.4	7.8	0.15	3.72	2.68
4	DL + LL + WL	18.23	97.8	11.6	0.12	3.72	2.7
5	DL + LL + EL	17.58	88.1	11.85	0.134	3.72	2.7

(7) Compute load factors α_{ij} and design load w_i.

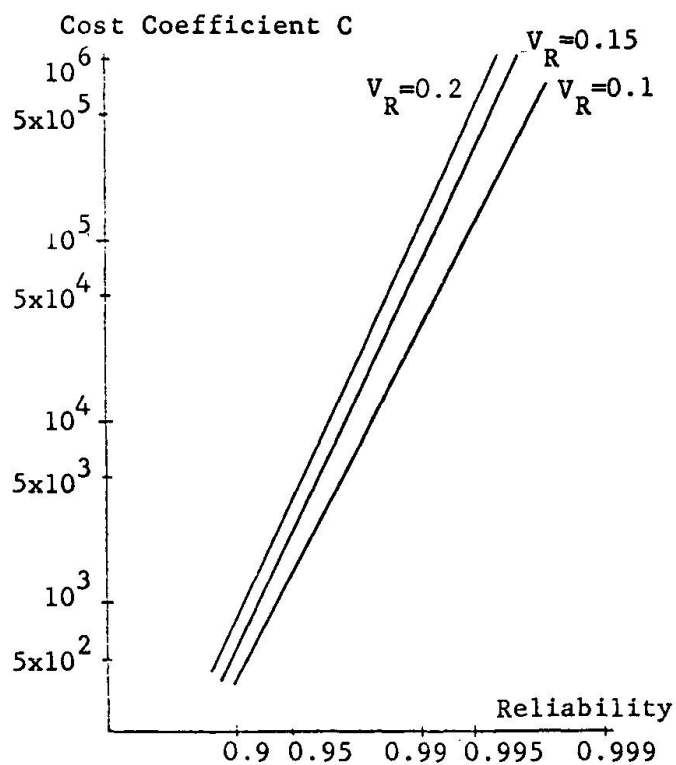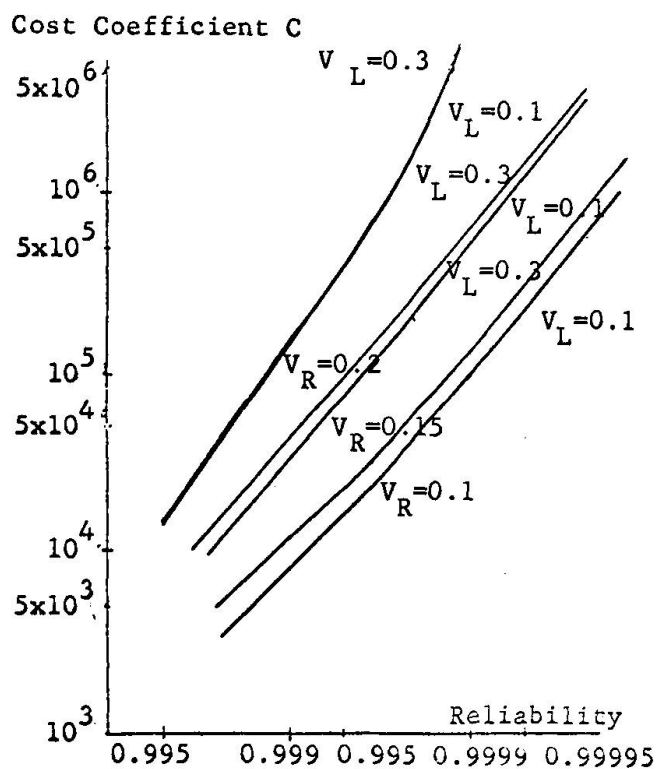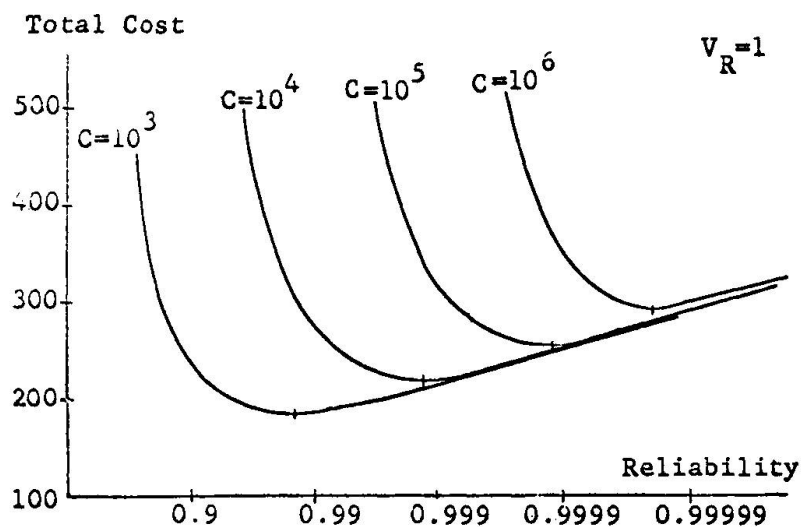| Case	Loading Combination	α_{i1}	α_{i2}	α_{i3}	α_{i4}	W_i(k-ft)
1	DL + LL	1.61	2.13	0	0	119
2	DL + WL	1.61	0	1.96	0	113
3	DL + EL	1.61	0	0	2.08	96.8
4	DL + LL + WL	1.57	1.97	1.85	0	177
5	DL + LL + EL	1.58	1.97	0	1.97	163

VII   Conclusion

An approach is presented in this paper to formulate a procedure for quantitative evaluation of load factors for dead, live, wind and earthquake loads. Various models which describe the statistical characteristics of the loads and resistance are studied under the formulation. Load factors obtained in each case for any desired level of reliability do not differ appreciably. The Gaussian

model for both the loads and resistance appear to be the most convenient one to work with. Step-by-step procedure are outlined to illustrate the simplicity in the evaluation of load factors. From system and cost analyses, the optimal level of reliability for the structural member design are mainly determined by two parameters. They are the cost coefficient C which represents the ratio of cost of failure and the cost of construction, and the coefficient of variation of resistance V_R. Once this desired reliability level is given, together with the coefficients of variation of each load component, the corresponding load factors may be computed by the procedures formulated.

References

1. Benjamin, J. R. and Lind, N. C., "A Probabilistic Framework for the Safety Provisions of the ACI Code," Symposium on the Application of Probabilistic Concepts to Strength Design of Reinforced Concrete Members, ACI Fall Conference. Memphis 1968.

2. Benjamin, J. R. and Nelson, M. F., "Tables of the Standardized Beta Distribution," Stanford University, Department of Civil Engineering, Technical Report No. 59, 1966.

3. Niyogi, P. K., "Application of Statistical Methods and Information Theory to Structural Reliability Estimates," Ph.D. dissertation, Department of Civil Engineering, University of Pennylvania, Philadelphia, Pa., 1968.

4. Niyogi, P. K., Shah, H. C., Doshi, K. D., and Tang, W., "Statistical Evaluation of Load Factors for Concrete Bridge Design," Second International Symposium on Concrete Bridge Design, April 1969, Chicago, Illinois.

5. Shah, H. C., and Benjamin, J. R., "Statistical and Probability Methods for Analysis and Design of Reinforced Concrete Structures," International Conference on Shear, Torsion and Bond in Reinforced and Prestressed Concrete. PSG College of Technology, Coinbatore, India, January 1969.

6. Shah, H. C., "The Rational Probabilistic Code Format," Symposium on the Application of Probabilistic Concepts to Strength Design of Reinforced Concrete Members, ACI Fall Conference, Memphis 1968.

7. Tang, W. H., "Statistical Evaluation of Load Factors in Structural Design," Stanford University, Department of Civil Engineering, Technical Report No. 103, 1969.

8. Recommended Lateral Force Requirement by Seismology Committee, Structural Engineers Association of California, 1959.

9. ASCE Task Committee on Wind Forces "Wind Forces on Structures (Final Report)", Trans. Am. Soc. Civil Engrs., 126 (II) pp. 1124-1198 (1961).
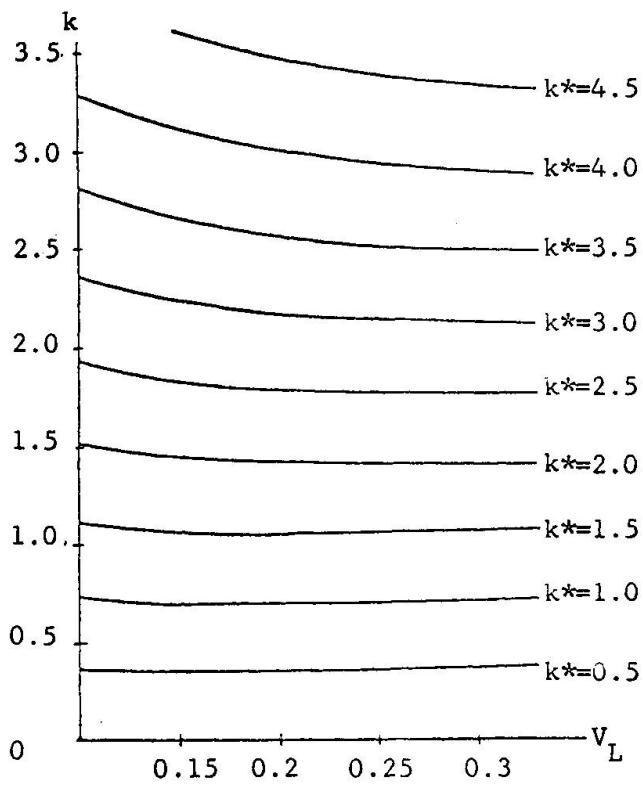
FIG. 1 TOTAL COST VS. ELEMENT RELIABILITY--
SERIES. SYSTEM

FIG. 2 COST COEFFICIENT VS. OPTIMAL
ELEMENT RELIABILITY--SERIES
SYSTEM

FIG. 3 COST COEFFICIENT VS. OPTIMAL
ELEMENT RELIABILITY--
PARALLEL SYSTEM

FIG. 4 CHART FOR DETERMINING
RELIABILITY COEFFICIENT
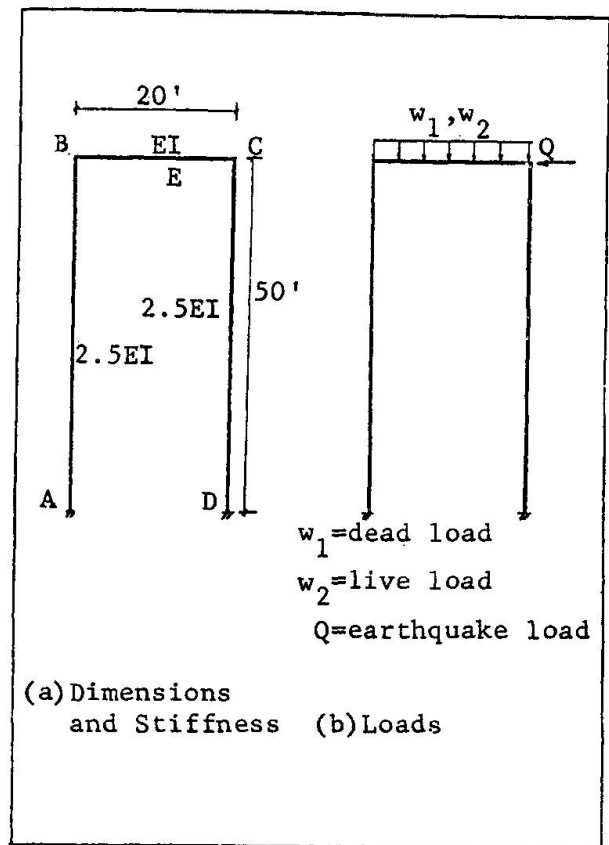k--V_R=0.15

(a) Dimensions
and Stiffness   (b) Loads

FIG. 5 PLANE FRAME EXAMPLE

Leere Seite

Blank page

Page vide

On Fatigue Damage Estimation of Railway Bridge Members Through Actual Train Loading

Sur l'estimation des dommages causés aux éléments de ponts-rails par la fatigue due aux essieux

Über die Schätzung von Ermüdungsschäden an Eisenbahnbrücken-Teilen durch Zuglasten

FUMIHITO ITOH
JAPAN

INTRODUCTION

The major load acting on railway bridges is the train load which makes a short-term variation. Its amplitude of variation is considerably wide, therefore in discussing the safety of railway bridge members it is important to consider not simply the maximum value of load but also the decline of strength due to repeated loading, i.e., the fatigue damage. It is for this reason that in many countries the specifications or codes for designing the railway bridges set an allowable unit stress for fatigue in bridge members, and information on how to decide the safe limit of fatigue strength is being eagerly sought by engineers.

Fatigue life depends on the number of repeated stress cycles as well as on the maximum value of stress. Therefore the thing to be known is not only what is the maximum value of stress developed under passage of a train but also to what number of stress cycles with an amplitude of the maximum stress in that condition corresponds the fatigue damage occurring in bridge members under passage of that train.

According to Prof. Pelikan, who investigated German trains, the number of repeated stress cycles mentioned above depends on the span length of a railway bridge. This trend must be the same with the Japanese railways, too. JNR has constructed Tokaido SHIN KANSEN as a line devoted to the operation of multiple-unit electric railcar trains. On this line, the train load is uniformly distributed but with a larger wheel base than in locomotives, the number of repeated loadings tends to be large. In case of bridges on SHIN KANSEN, with the above fact taken into account, the designing was so made as to let the bridge bear a larger load than really encountered but the difference due to bridge span length was ignored.

The purpose of this paper is to investigate the situation in more

detail.   The points to be elucidated are: How best to analyze the
stress-time relation; how best to utilize the results of this analysis
for estimation of fatigue life; how to relate these results to train
category or span length of a bridge; or what are the best statistical
quantities for checking the safety.   The present paper sums up what has
so far been achieved on this problem by the author in his own way which
is even short of the statistical approach.

STRESS-TIME RELATION UNDER TRAIN LOAD

The stress-time relation developing in bridge members under train
passage has different features from those of airplane wings in turbulent
air or of axles in running cars.   The stress in a wheel axle varies
randomly on both sides of the mean level which is virtually constant,
with no definite correlation existing between maximum and minimum.
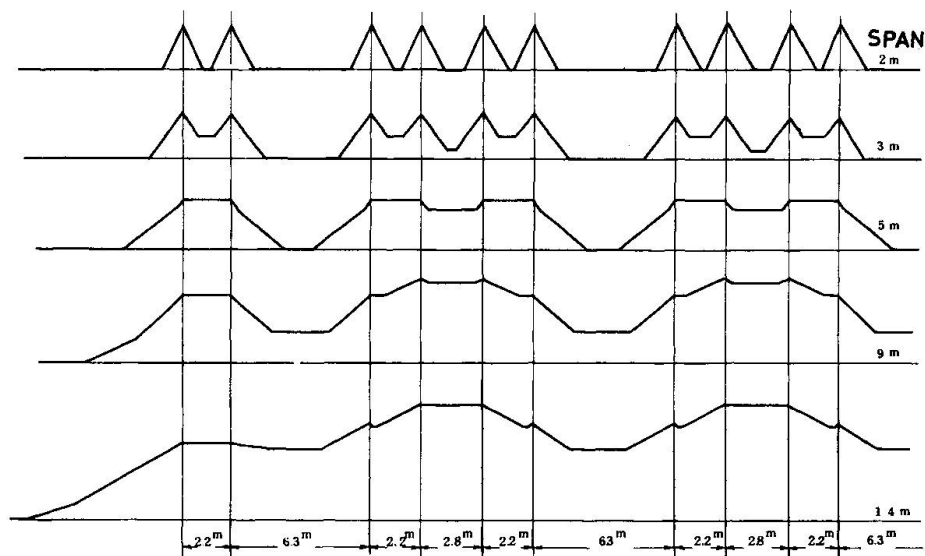

Fig. 1   Theoretical stress-time relations
under Tokaido SHIN KANSEN N-load train.

By contrast, the stresses in bridge members are, though short in
duration, characterized by mean stress variation which has a stress-time
relation depending on train category, span length of the bridge and
functions of members, and a relatively small oscillation added around
this stress.   Figure 1 illustrates the theoretical wave form appearing
Tokaido SHIN KANSEN passes over simple supported girders of several
different span lengths, the wave form is broadly similar to the above-
mentioned mean stress variation.   From this it is realized how influen-
tial is the span length.

STATISTICAL COUNTING METHODS FOR ANALYZING LOAD-TIME HISTORIES TO BE
APPLIED FOR ESTIMATION OF FATIGUE LIFE

In the discussion of fatigue life, it is not enough to find simply
the magnitude of maximum stress intensity and its probability of occur-
rence.   Because the fatigue strength is not associated with the magni-
tude and frequence of maximum stress intensity only, but, more important,
with those of stress amplitude.   Thus, the counting method for this
purpose must be one that can permit conversion to the magnitude and

frequence of stress amplitude so that the counted stress waves appear-
ing in railway bridge members may be related to the fatigue strength.
If several such methods are available, the most reasonable and most
practicable one must be selected from among them.

The author checked the following nine as such counting methods:
a) Peak Count Method.
b) Mean-Crossing Peak Count Method.
c) Level-Crossing Count Method.
d) Fatigue Meter Count Method.
e) Range Count Method.
f) Range-Mean Count Method.
g) Modified Range Count Method.
h) Range-Pair Count Method.
i) Modified Range-Pair Count Method.

Out of these nine, the four (a)-(d) are rejected for the present
purpose because they cannot give stress amplitude from counted result on
stress-time relations such as developed in railway bridges. The methods
(e) and followings, which deal with stress amplitude from the first, are
satisfactory in this respect, but the other three except (h) and (i)
have the drawback that not only the results vary depending on the
position and number of artificially selected counting levels, but also
a major amplitude is apt to be overlooked as the result of minor
vibration components, if any, being counted. Since it is undesirable
to adopt for the solution of a scientific problem a method whose data
depend on something artificial, the author thinks it advisable to
refrain from use of such methods.

The remaining two methods (h) and (i) produce absolutely the same
results. The instruments available for Range-Pair Count Method have a
slow response, and to count the stress so rapidly changing as those in
railway bridge the instrument becomes too large to be fit for field use.
Thus, Modified Range-Pair Count Method has been found best for this
purpose.

This is a method devised by Shiraishi; in this method the maximum
and minimum values in stress-time relation are arranged in the order of
their occurrence and they as reduced to a pulsating load are counted.
Shiraishi performed the reduction graphically, but the author changed
the procedure to do it numerically with no resort to the counting level.
Measured stress-time relations are recorded on magnetic tape and, after
reduced by the data processor to a series of extreme values, are fed to
the electronic computer for necessary conversion.

METHOD TO BE USED FOR ESTIMATION OF FATIGUE LIFE

Numerous studies have been made to search for a damage law that can
predict the number of repeated cycles to failure of members subjected to
variable load such as to be able to agree with experimental results, but
there is yet no theory established about which of these studies can give
the most re liable results.

Here the author is going to discuss not in terms of determining
which of these studies is generally the most accurate but in those of
finding which of them will be the most convenient for the practical
purpose. In this line of thinking certain errors would be tolerated.

From this standpoint the so-called Miner's method or its improvement, for instance, method of Corten & Dolan seems to be the most preferable one. As steel, when corroded, has its endurance limit reduced, here for the purpose of simplifying the calculation, the endurance limit of steel is to be disregarded.

Then putting the stress in a material as σ_i , its number of cycles to failure at this stress level as N_i and k as a constant, it is assumed that the following holds:

$$\sigma_i N_i^k = \sigma_j N_j^k .$$

Under this assumption a fatigue failure occurs when the following holds:

$$\sum_i \left(\frac{n_i}{N_i} \right) = 1.0 .$$

If the number of stress amplitudes σ_i appearing under passage of one train as live load is n_i' , the number of trains, N_t , to a fatigue failure will be:

$$\frac{N_t}{N_1} \sum_{i=1}^{m} n_i' \left(\frac{\sigma_i}{\sigma_1} \right)^{1/k} = 1.0 .$$

Therefore, if

$$N_{e1} = \sum_{i=1}^{m} n_i' \left(\frac{\sigma_i}{\sigma_1} \right)^{1/k} ,$$

N_t will be given as the ratio of repeated numbers N_1 and N_{e1} to the representative stress σ_1. If the maximum stress due to a train load is taken as representative stress σ_1 and if the values of a different reference stress σ^* and the repeated number N^* corresponding to this stress are known, N_t will be given by

$$N_t = \frac{N^*}{N_{e1}} \left(\frac{\sigma^*}{\sigma_1} \right)^{1/k} .$$

If the number of trains in category j passing over the bridge in one year is n_{tj} , σ_1 for jth train category is σ_j , etc., and the number of train categories are s, the serviceable number of years T for the bridge will be given by

$$T = \frac{N^*}{\sum_{j=1}^{s} n_{tj} N_{ej} \left(\frac{\sigma_j}{\sigma^*} \right)^{1/k}} ,$$

or finding the equivalent maximum stress intensity for each train, i.e., $\sigma_t = \sigma_1 N_{e1}^k$, T will be given by

$$T = \frac{N^*}{\sum_{j=1}^{s} n_{tj} \left(\frac{\sigma_{tj}}{\sigma^*} \right)^{1/k}} .$$

If σ_t follows a logarithmic normal distribution with σ_m as median, putting the total number of trains in a year as N_0 and using the

standard deviation S_0 of log δ_t the following is calculated:

$$N_{eq} = N_0 \; exp\left[\frac{S_0}{2\,k^2}\right] \, ,$$

and accordingly will be found as

$$T = \frac{N^*}{N_{eq}} \left(\frac{\delta^*}{\delta_m}\right)^{1/k} .$$

ESTIMATION BY STATICAL CALCULATION

As mentioned above, the fatigue damage under train passage depends on the equivalent repeated cycles N_{e1} as well as on the magnitude of maximum stress. Much attention has been paid to the maximum stress, but N_{e1} is an entirely novel conception and the following discussion will center around N_{e1} .

(1) Bridge Span vs. Train Categories.
Calculations were made with four categories of train and the relations between the number of trains in each category that can be passed until failure of bridge members and the span length of bridge was established as in Fig. 2. The categories of trains adopted for calculation and their symbols were as follows:

Fig. 2. Span-life relations by statical calculation.

a. 30 x N; Standard freight electric railcar train for designing Tokaido SHIN KANSEN, composed of 30 cars.
b. 12 x P; Standard passenger electric railcar train for designing Tokaido SHIN KANSEN, composed of 12 cars.
c. 12 x P'; Revenue passenger electric railcar train operated on Tokaido SHIN KANSEN, composed of 12 cars.
d. K18 + 30F; A locomotive of K18 standard construction load in Japan hauling 30 four-axle freight cars 10m long with 15 ton axle weight.
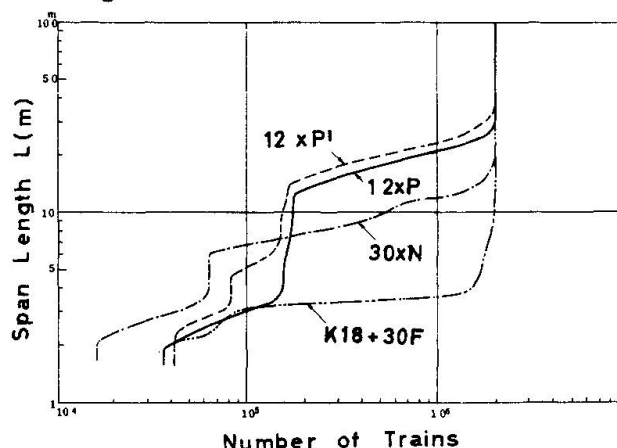
Bridge members considered in this calculation were cord members at span center or flange with k = 0.20 taken on assumption that they were designed to be able to stand just 2 million loadings at maximum stress.

From these calculations it may be concluded:
a) N_{e1} of a girder with shorter span length than the shortest wheel base is practically equal to the number of axles and constant regardless of span length.
b) For a train hauled by a heavy locomotive, practically N_{e1} = 1.0 will hold, if the span length of the bridge is longer than 4m.
c) For an electric railcar train, too, $N_{e1} \doteqdot 1$ .0 will hold, if the bridge span length is more than 1.3 ~ 1.5 times the car length.
d) Under an electric railcar train, N_{e1} is approximately equal to the number of car couplings on a girder with a span longer than the wheel-base at the coupling and shorter than the wheel-base between the second and the third axles of a car.

(2) Difference Depending on Position of Section Under Consideration.

So far as the bending moment is concerned, the value depends little on the position of the member considered in the axial direction of bridge. The results of calculations about 7 sections in a span under passage of JNR series 181 10-units electric car train fitted all into the shaded region in Fig. 3.

(3) Load-Spreading Effect of Rails.

In JNR, there has never been a single case of even a short-span bridge developing a fatigue failure in its members. This may raise a doubt about the reliability of the above theory.

If the bridge is supposed to have been designed to have a strength that can stand for 2 million repetitions of loading in accordance with the castomary practice and the axle weight is assumed to be spread actually as Fig. 4 on account of rail- and sleeper rigidity, the calculation about the same train as in Fig. 2 produces the results as indicated in Fig. 5.
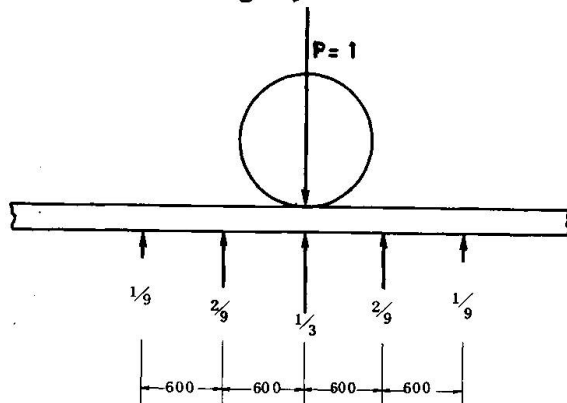
Fig. 3. L - N_t curve of simple girder under 10 units car train (Series 181).

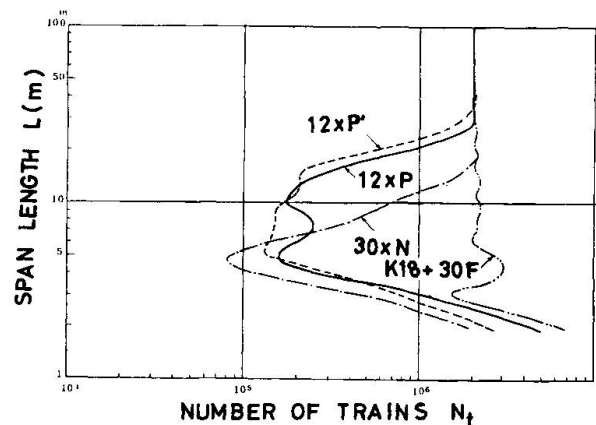Fig. 4. Assumed distribution of load under sleepers.

Fig. 5. L - N_t curve under effect of rail and sleeper rigidity.

Namely, so long as the bridge has been customarily designed and the rails supported by the sleepers, the hazard of fatigue failure in a span shorter than 4 m may be rather discounted. Thus, it may be practically presumed that a train hauled by a heavy locomotive necessarily developes a maximum stress intensity only once in its passage. Concerning the electric railcar trains, bridges calling for the most elaborate checking exist in the range of span lengths between 4 m and 20 m.

ANALYSIS USING MEASURED WAVE FORM

Real stress waveforms emerging in bridges are not always in agreement with the results of customary calculations. As well known, all stress-time relations make a smooth charge with no inflections such as

observed on calculated curves. Meanwhile, an increased train speed is accompanied with a vibration which is not susceptible of routine calculation. Thus it becomes necessary to ascertain to what extent the above-mentioned calculation is applicable to the real waveforms. Here are to be cited a few examples in recent times.
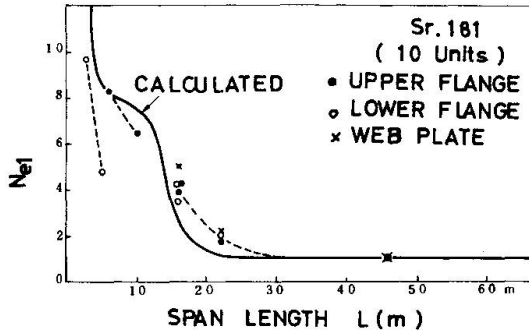
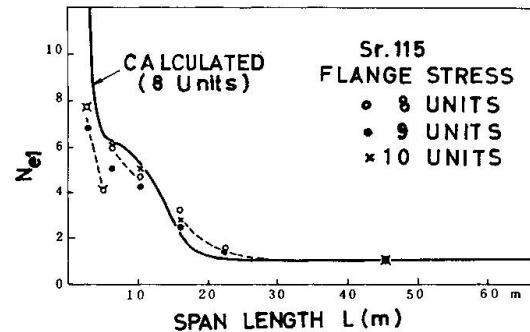Fig. 6. $L \sim N_{e1}$ relation by electric railcar train (Series 181, 10 units).

Fig. 7. $L \sim N_{e1}$ relation by electric railcar train (Series 115) measured on flanges of girder.

Fig. 6 and Fig. 7 illustrate the $L \sim N_{e1}$ relations as obtained from a similar analysis to the above of measured stresses in three plate girders, respectively with span lengths of 16.0m, 22.3m and 45.5m, in these figures, in addition to the data on the main girders, data using the measured stresses in 3.2m and 5.1m stringers as well as cross beams 6.4m and 10.2m long in the influence line are entered. Cross beam may be equated to main girder, but the curve for stringer characterized by continuity cannot agree with the curves plotting the results about main girders or cross beams.
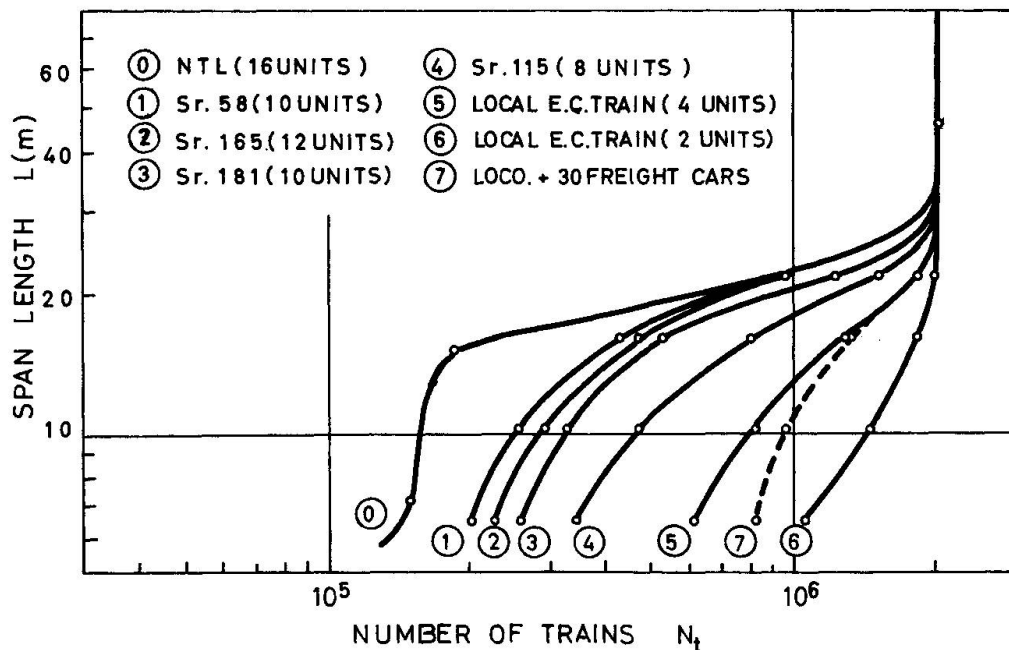
Fig. 8. Relation between span length and number of train passage to failure.

Figure 8, summerizing the results of such measurements, illustrates the relation between span length and number of train passages to failure just like in figure 2. Thus it can be said that the results of analysis based on measured waveforms are in the same tendency as the results of static calculations. So far as the range measured here is concerned, a slight difference in the stress-time relation and the small amount of vibration seem to have no large bearing on fatigue.

This, however, does not mean that N_{el} is not sensitive to the speed. The author has some data which show extremely great influence beyond certain critical speed. In spite of these results, nothing conclusive can be said about the general tendency in the effect of speed on N_{el}, because even among girders looking similar, some are influenced heavily by the speed, and others are little influenced by it, while still others are almost free from the influence of speed.

After all, above-mentioned equivalent numbers of loading, instead of crude statistical distributions of counted data on stress-time relations in railway bridges, seems to have a merit or possibility to be used as one of statistical quantity to measure the remaining life to fatigue failure under actual train loadings.

REFERENCES

(1) Pelikan W. "Eine Betrachtung über die Größe der Betriebslasten von Eisenbahn- und Straßenbrücken und ihre Auswirkung auf die Bemessung dieser Bauwerke", Der Bauingenieur, Nr.43, Heft 6, ss.207-214, 1968.

(2) Schijve J. "The Analysis of Random Load-Time Histories with Relation to Fatigue Tests and Life Calculations", Fatigue of Aircraft Structures, Symposium Publication Division, Pergamon Press, pp.115-149, 1963.

(3) Shiraishi T. "Life Calculation Method for Welded Joint", Preprint of Symposium on Fatigue of Materials, Japanese Society of Welding, p.47, 1963 (in Japanese).

SUMMARY

A kind of fatigue life estimating method combining that of Corten and Dolan with modified range-pair count method is suggested, which is practical to calculate the fatigue damage of existing railway bridge members.

The result of the illustrative applications of this method on simply supported girders shows that equivalent numbers of loading cycle depend on the span length of the girder and the arrangement of the wheel axles.

RESUME

L'auteur présente une méthode pour prédire la résistance à la fatigue des éléments de ponts ferroviaires. Il s'agit de la combinaison de deux méthodes; l'une permettant d'évaluer la limite de fatigue, proposée par Corten et Dolan, et l'autre étant une modification de la "range-pair count method".

Les résultats d'application de cette méthode à la poutre simplement appuyée nous montre que la fréquence équivalente des charges dynamiques dépend considérablement de la portée de poutre et de la répartition des essieux du train.

ZUSAMMENFASSUNG

Für die Ermüdungsdauer wird eine Schätzmethode, jene von Corten und Dolan mit dem abgeänderten Verfahren des "Schwingungsweite-Zählens" kombinierend, vorgeschlagen, die erlaubt, das Ermüdungsversagen für Eisenbahnbrückenteile einfach zu berechnen.
Das Ergebnis der Anwendungen auf einen einfach aufgelegten Träger zeigt, dass die Anzahl Lastwechsel von der Trägerspannweite und der Radachsenanordnung abhangen.

Leere Seite

Blank page

Page vide

Aspects statistiques concernant les surcharges climatiques et la sécurité des constructions

Die statistische Seite der Klimabelastung und der Bauwerkssicherheit

Statistic Aspects on the Climatic Loadings and the Safety of Structures

A. NEGOIŢĂ   A. IANCĂU
Prof. Ing.   Conf. Ing.
Roumanie

L'étude de la sécurité des constructions [2],[5], [15],[22], [19], et des surcharges climatiques [1],[3],[4],[6],[9],[12],[13], [14],[17],[20],[21] ont été l'objet de nombreuses recherches. Les hommes de science ont cherché à déterminer avec exactitude les surcharges qui agissent sur les bâtiments et les efforts dans les éléments des bâtiments, pour pouvoir envisager un coefficient de sécurité minimal, qui ne compromette pas la résistance, la sta-bilité et les conditions d'exploitation des bâtiments.

Les nouvelles méthodes et les possibilités d'exécution ont permis de réaliser des toitures légères ayant un petit rapport poids propre sur grandeur des surcharges climatiques, ce qui augmente l'importance relative des surcharges climatiques.

Quand on néglige la possibilité des accumulations maximales de neige [9],[10], de son épaisseur maximale probable [13],[14], ou de la vitesse maximale du vent [12],[15], on risque l'écroule-ment partiel ou total ou la perte de la stabilité lors de l'ex-ploitation.

Dans notre pays, le Prof.Dr.Ing. Cristea Mateescu, membre correspondant de l'Académie, a entrepris des recherches très in-téressantes au sujet des accumulations de neige sur les toitures par l'action du vent, en effectuant des essais sur modèles dans un tunnel aérodynamique avec des matériaux pulvérulents et en établissant les critères des similitudes mécaniques [9].

En même temps, le Dr.Ing. Horia Sandi a effectué des études concernant la sécurité des constructions soumises aux surcharges temporaires à l'aide du calcul des probabilités, spécialement pour les toitures légères avec différentes durées d'exploitation [19].

Dans le calcul des constructions à l'état limite, on tient compte de la variabilité dans la qualité des matériaux, les char-ges et les surcharges, et dans les conditions de travail, en sé-parant le coefficient unique de sécurité en trois coefficients divers, à savoir les coefficients de surcharge n, d'homogénéité k, et des conditions de travail m (à l'aide duquel on réduit soit la résistance des matériaux m_m, soit la capacité portante de l'élé-ment m_e).

La liaison entre la valeur du coefficient unique (c) et les coefficients diversifiés (n, k, m_m, m_e) peut être exprimée par la relation [11] :

$$c = \frac{n}{m_m \, m_e \, k} \qquad (1)$$

ou quand $m_m = 1$

$$c = \frac{n}{m_e \, k} \qquad (2)$$

Pour vérifier un élément constitué d'un matériau homogène, on peut employer la relation:

$$\sum n \, S^n \leqslant m_e \, m_m \, k \, R_F^n \qquad (3)$$

dans laquelle F est la caractéristique géometrique de la section de l'élément considéré. Dans le cas de l'élément exécuté à l'aide de plusieurs matériaux, cette relation devient:

$$\sum n \, S^n \leqslant m_e \, m_m \, k_i \, R_i^n \, F_i \; . \qquad (4)$$

Les résistances de calcul sont données dans les prescriptions techniques et quand on tient compte des conditions de travail des matériaux, cette relation a la forme:

$$\sum n \, S^n \leqslant m_e \sum R_i \, F_i \qquad (5)$$

qui, dans le cas plus général où m = 1, devient

$$\sum n \, S^n \leqslant \sum R_i \, F_i \; . \qquad (6)$$

La somme des sollicitations normées multipliées par le coefficient de surcharge, nommée sollicitation de calcul $\sum n \, S^n = S$, représente la sollicitation maximale possible.

Les normes françaises "élaborées par la Commission des spécialistes français sous la présidence de Monsieur N. Esquillan" considèrent comme surcharge normale la surcharge qui peut être atteinte une ou plusieurs fois dans l'année, et comme surcharge extrême la surcharge atteinte une seule fois pendant la durée de service de la construction.

On a fait des études statistiques pour les surcharges climatiques (vent et neige) [12] , [13], [14], [15] , en utilisant les observations météorologiques enregistrées [23]. Les fonctions de distribution théoriques qui correspondent le mieux à la distribution empirique des surcharges climatiques sont celles de Fisher-Tippot, de Gumbel, la fonction logistique, exponentielle, la loi de Poisson et de Pearson. On a obtenu des résultats convenables avec la méthode de Gumbel, appliquée aux surcharges climatiques en utilisant les études théoriques de Monsieur G. Demarre [3].

La vitesse maximale du vent à Bucarest-Filaret a été étudiée en utilisant une série d'observations de longue durée (65 années); la valeur maximale enregistrée est de 41,9 m/s et la moyenne de
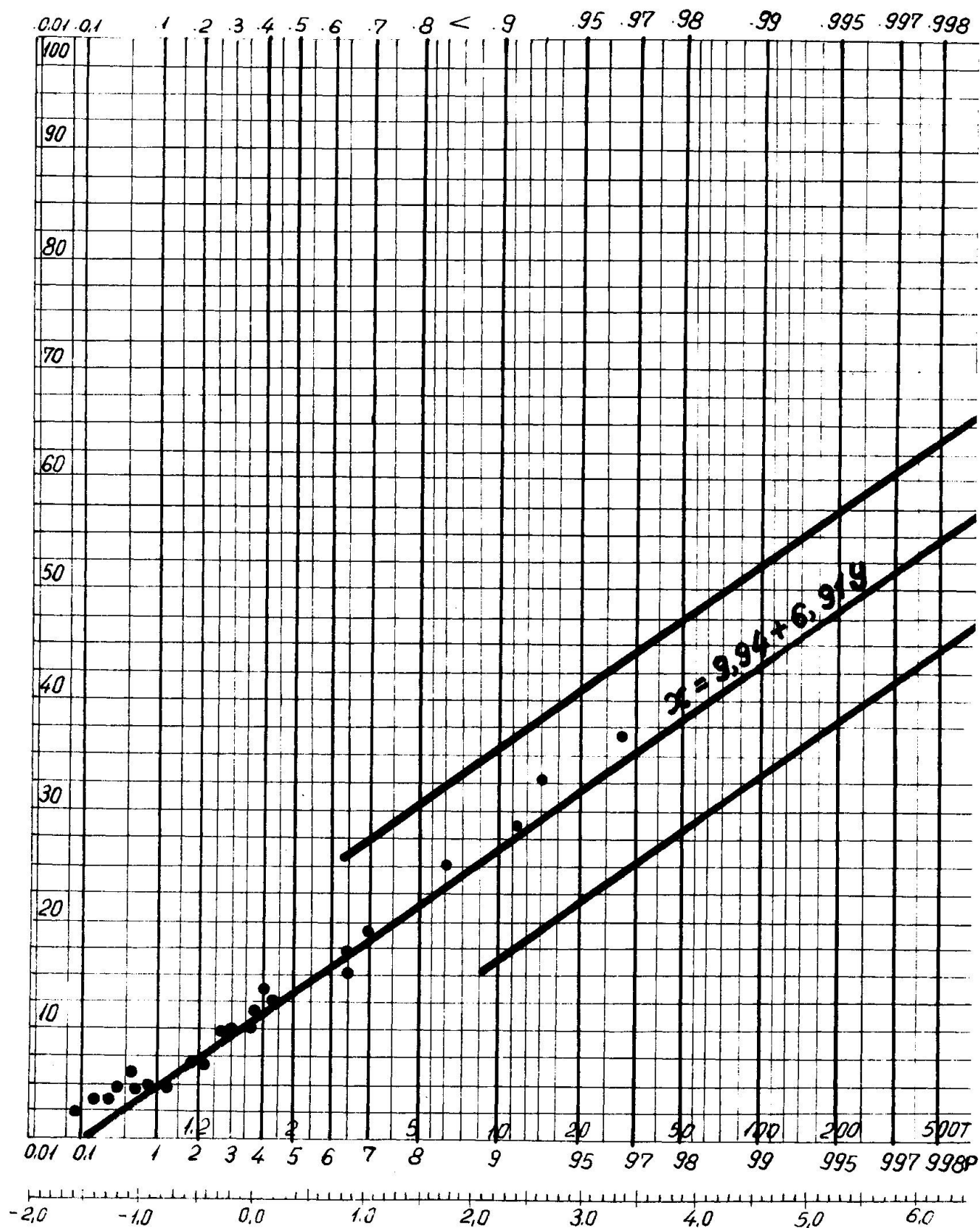
Fig. 1 La droite de Gumbel pour la vitesse du vent à Bucarest-Filaret

13,74 m/s (fig. 1).

A l'aide de la droite de Gumbel, nous avons fait des extrapo-
lations pour différentes périodes de temps, en calculant à l'aide
de la formule de Newton les valeurs correspondentes de la pression
dynamique de base.

Dans la littérature spécialisée, on prend en général la valeur
1,2 pour le coefficient de surcharge n des bâtiments habituel [16].
Pendant les 65 ans d'observation, cette valeur a été dépassée en
atteignant un coefficient de surcharges 1,57. On mentionne que les
normes françaises indiquent un rapport entre la pression dynamique
normale et extrême de 1,75 [18].

Pour la surcharge de neige, on a analysé deux aspects: l'épais-
sur maximale probable de la couche de neige et la densité volumé-
trique de la couche de neige.

On a évalué l'épaisseur maximale probable de la couche de neige
à Bucarest-Filaret en utilisant les observations effectuées pendant
48 ans. La valeur maximale enregistrée sur le terrain a été de 150
cm et la moyenne seulement de 47,5 cm. On prend pour la surcharge
due à la neige un coefficient de surcharge n = 1,4. Les normes fran-
çaises [18] prennent 1,65 pour le rapport entre la surcharge extrême
et la surcharge normale. Le poids de la neige pour 1 m² de surface
horizontale dépend naturellement de la densité volumétrique de la
neige et de son épaisseur.

L'Institut Météorologique Central de Bucarest a effectué ces
dernières années des enregistrements systématiques de la densité
volumétrique de la neige. La moyenne de la densité maximale men-
suelle était 0,255 t/m³, le maximum maximorum de 0,74 t/m³ étant en-
registré exceptionnellement au mois de février 1968. Au mois de jan-
vier 1969, la densité volumétrique de la neige sur les toitures à
Bucarest a atteint 0,30 - 0,55 t/m³. On peut accepter pour la neige
tombée successivement pendant l'hiver une densité volumétrique de
0,22 t/m³ [11], en apportant des corrections à l'aide du coefficient
de surcharge n et en fonction de la durée de service de la construc-
tion et du mode de l'action (direct, indirect etc.) de la neige sur
l'élément de construction.

Les dernières recherches astronomiques font une liaison entre
les éléments climatiques de la terre et le soleil; les éruptions du
soleil, etc. On remarque dans les phénomènes solaires l'existence
de cycles ayant des durées différentes: le plus connu est de 11 ans,
et son existence a été marquée dans notre pays par des hivers excep-
tionnels (fig. 2), 80 et 400 ans sont aussi des cycles dont l'exis-
tence a récemment été étudiée. Nos observations météorologiques ne
contiennent pas encore un si grand intervalle de temps et on cherche
maintenant à utiliser les méthodes statistiques mentionnées plus
haut pour l'étude de la variation de longue durée de phénomènes so-
laires.

On emploie en général dans divers pays la classification des
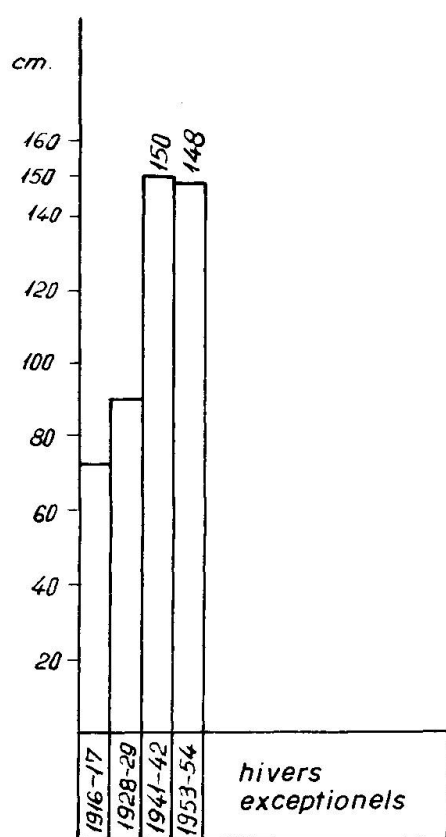bâtiments d'après leur durabilité; on distingue trois catégories de

de bâtiments caractérisées par des durées de 20, 50 et 100 ans. On peut calculer différentes valeurs du coefficient de surcharge n, selon la durée d'exploitation de 20, 50 ou 100 ans, en fonction des enregistrements statistiques.

Il en résulte, par exemple, comme surcharge maximale extrême dans la zone de la ville de Bucarest, un coefficient de surcharge de 1,50 pour une durée de 80 ans, alors que la valeur utilisée dans quelques prescriptions est de 1,2. Les mêmes considérations peuvent être valables pour la surcharge extrême due à la neige. Il en résulte ainsi la nécessité d'établir les maxima maximorum (extrêmes) des surcharges climatiques pour un bâtiment, en fonction de 20, 50, 100 ans ou plus, et de la valeur des surcharges.

Fig. 2 L'épaisseur maximale de la neige lors des hivers exeptionels à Bucarest – Filarest

Evidemment il faut tenir compte du fait que les valeurs établies à l'aide des données statistiques doivent être appliquées différemment selon l'importance de l'élément de construction (principal ou secondaire), c'est-à-dire en fonction du mode d'application ou de transmission de la surcharge climatique, directement ou par l'intermédiaire d'autres éléments. Dans le cas des éléments de construction indirectement sollicitées, il faut faire des réductions correspondantes, différentes dans le cas de la neige ou du vent.

Pour le calcul des constructions soumises à l'action des surcharges climatiques, le rapport entre la charge accidentelle (surcharge) et le poids propre de l'élément (poids mort) présente aussi une certaine importance. Les études effectuées par le Dr.Ing. Horia Sandi [19] ont abouti à différentes valeurs du coefficient de sécurité des toitures (fig. 3), en fonction de la durée d'exploitation de la construction T, et du rapport Z^n/P^n (poids de la neige/poids propre de la toiture).

Dans le cas de la surcharge due à la neige, il faut aussi tenir compte de la possibilité de l'accumulation de la neige qui dépend de la forme de la toiture, de l'action du vent et des autres facteurs. On notera que la forme architectonique des toitures légères, qui peut très largement varier, est importante pour la surcharge due à la neige; l'étude sur modèle établie par le Dr.Ing.
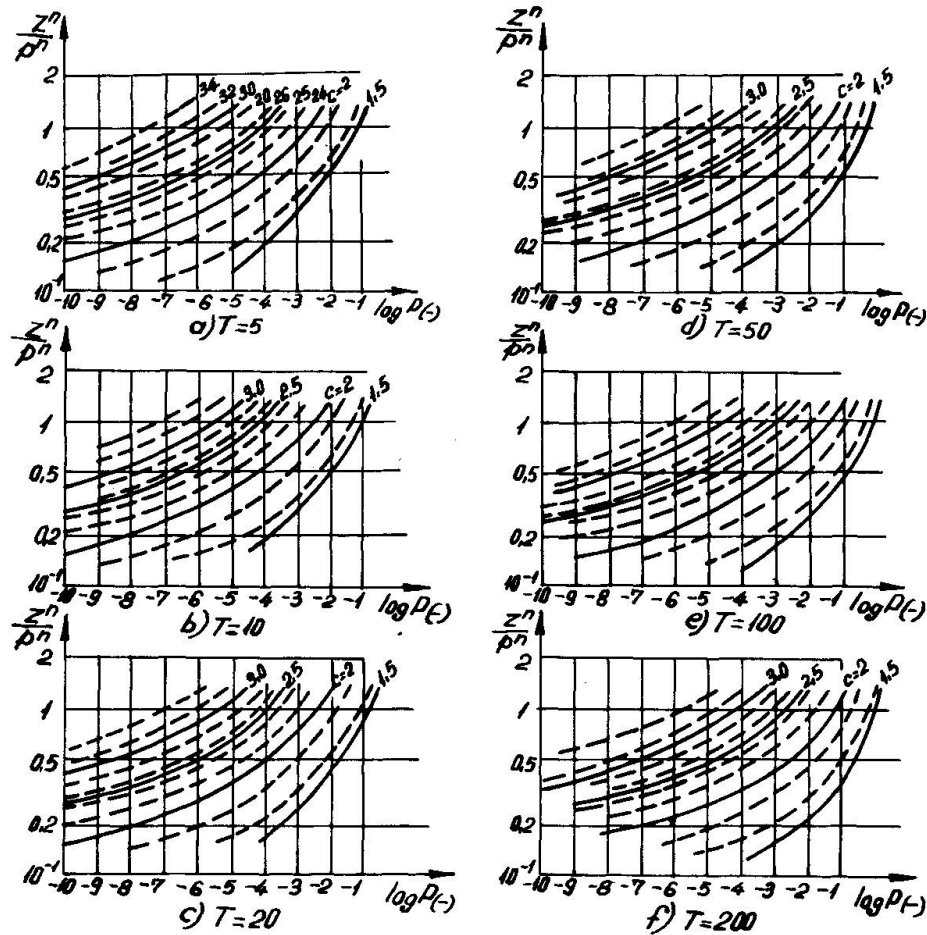
Fig. 3   Courbes des coéfficients de sécurités

Cristea Mateescu peut être appliquée avec une certaine exactitude dans ce cas [9] .

L'étude statistique des phénomènes météorologiques permet de déterminer les surcharges climatiques maximales probables pour la durée convenable de 20, 50, 100 ans ou plus. On peut ainsi utiliser pour les bâtiments des coefficients de surcharges différents pour 20, 50, 100 ans ou plus.

Bibliographie

[1]   Borges, J.F.,   Sollicitations dynamiques (particulièrement dues au vent et aux séismes), Association Internationale des Ponts et Charpentes, Huitième Congrès, New-York 9-14 sept. 1968.

[2]   Carpena, A.,   Calcul probabiliste des structures métalliques, Paris, Constructions métalliques No 1/1967.

[3]   Demarre, G.,   La loi de Gumbel et son application à la détermination des surcharges climatiques extrêmes, Paris, 1966.

[4]   Esquillan, N.,   Les effets de la neige et du vent sur les constructions et les règles N.V. 65, Annales de l'Institut Technique du Bâtiment et des Tra-

vaux Publics, No 250, oct. 1968, Paris.

[5] Freudenthal, A.M., Etude critique des critères de sécurité
et de leurs fondements conceptuels, Associa-
tion Internationale des Ponts et Charpentes,
Huitième Congrès New-York, 9-14 sept. 1968.

[6] Guérin, P., Mesure de l'effet du vent sur les bâtiments de
grande envergure, Paris, 1962.

[7] Guillot, M., Le poids de la neige en plaine, Communication
à la Société Hydrotechnique de France, Section
de Glaciologie, Paris, 1967.

[8] Kostin, S.I., Pokrovskaia, T.V., Climatologie, București 1964.

[9] Mateescu, C., Contribuții la studiul aglomerării cu zăpadă
pe construcții sub acțiunea vîntului. Nr. 3
Tomul 18/1963.

[10] xxx Monografia geografică a R.P.R., București,
Editura Academiei, 1960.

[11] Negoiță, A., Drogeanun N., Clădiri civile, I, București
E.D.P. 1964.

[12] Negoiță, A., Iancău, V., Aspecte statistice ale încărcării
dată de vînt, comunicare la sesiunea științi-
fică a cadrelor didactice de la Institutul Po-
litehnic Cluj, oct. 1968.

[13] Negoiță, A., Iancău, V., Considerații asupra încărcării dată
de zăpadă, comunicare la sesiunea științifică
a cadrelor didactice de la Institutul Politeh-
nic din Iași, sept. 1967.

[14] Negoiță, A., Iancău, V., Etudes statistiques concernant les
surcharges de neige à Cluj -République So-
cialiste Roumanie, 1968.

[15] Negoiță, A., Iancău, V., Contribuții privind aspectele pro-
babilistice ale încărcărilor climatice și si-
guranța construcțiilor, comunicare la Conferin-
ța Națională de Mecanică Aplicată organizată
de Academia R.S.R., București 24-27 iunie 1969.

[16] xxx Normativ condiționat pentru calculul construc-
țiilor la stările limită. P. 6-62, P. 7-62,
P. 8-62, București, Ed. Tehnică 1963.

[17] Pyschykov V.G., Methods for consideration of Variation and
Probability of combination of Wind, Snow and
Vertical Crane Loads, Kiew, 1967.

[18] xxx Règles définissant les effets de la neige et
du vent sur les constructions.

[19] Sandi, H., Asupra siguranței construcțiilor supuse încăr-
cărilor temporare, studii și cercetări de me-
canică aplicată, Nr. 5, tomul 23/1966.

[20] Sfintesco, D., Effets du vent sur les ossatures métalliques,
Mémoires, Association Internationale des Ponts
et Charpentes, 26e volume, 1966.

[21] Sfintesco, D.,   Résistance aux actions dynamiques du vent, et des séismes, Association Internationale des Ponts et Charpentes, Huitième Congrès, New-York, 9-14 sept. 1968.

[22] Steletki, A.S., Bazele calculului statistic al coeficientului de siguranţă a construcţiilor, Moscova, Gosstroizdat, 1947.

[23] xxx   Buletinul observaţiilor meteorologice din România.